



Integration of Soil Shear Strength Analysis with Wave Force Calculations to Optimize Coastal Slope Stability

EDY SOESANTO^{1,2}, DICKY MUSLIM¹, EVIE HADRIJANTIE SUDJONO³, and CIPTA ENDYANA¹

¹Faculty of Geological Engineering Universitas Padjadjaran
Jln. Dipati Ukur No. 35, Bandung, West Java 40132, Indonesia

²Universitas Bhayangkara Jakarta Raya

Jln. Raya Perjuangan No.81, Marga Mulya, Kec Bekasi Utara, Kota Bekasi, Jawa Barat 17143

³Research Center for Geological Disaster, National Research and Innovation Agency
Jln. Sangkuriang, Bandung 40135, West Java, Indonesia

Corresponding author: edy22001@mail.unpad.ac.id

Manuscript received: April, 17, 2024; revised: June, 11, 2024;

approved: April, 19, 2025; available online: June, 10, 2025

Abstract - Coastal regions face significant challenges due to the dynamic interplay between waves and soil slopes, which can lead to instability and erosion. This study investigates the stability of coastal slopes under wave-loading conditions by integrating soil shear strength analysis with wave-induced forces calculation. The simplified slope stability analysis method serves as the framework for assessing slope stability, while wave characteristics such as height, period, and direction are considered to calculate driving forces induced by waves. Soil shear strength parameters, including cohesion and friction angle, are incorporated to determine the resisting forces within the soil mass. An example scenario illustrates the calculation process, demonstrating how wave shear stress and soil shear strength interact to influence slope stability. This research found that wave parameters such as height, period, and direction had a significant influence on the magnitude of the driving force acting on the coastal slope. The distribution of wave pressure and wave forcing is also described, showing a significant increase in pressure at certain depths. This research resulted in the integration of soil shear strength with calculations of forces caused by waves, which greatly influenced the stability of coastal slopes. This research shows that soil with higher shear strength has better resistance to forces caused by waves. Coastal slopes with a FoS value of more than 1 are considered stable, while slopes with a FoS of less than 1 indicate instability and potential failure. At a certain depth, driving forces are dominant, which increases the potential for slope failure. The main innovation of this research is the approach that combines hydrodynamic analysis with geotechnical analysis to assess coastal slope stability, the simplified slope stability method approach from Bea and Audibert (1981) to calculate FoS on coastal slopes, and the use of Historical Data and Numerical Modeling for Force Evaluation Wave.

Keywords: wave-induced, soil shear strength, driving forces, resisting forces, the factor of safety

© IJOG - 2025

How to cite this article:

Soesanto, E., Muslim, D., Sudjono, E.H., and Endyana, C., 2025. Integration of Soil Shear Strength Analysis with Wave Force Calculations to Optimize Coastal Slope Stability. *Indonesian Journal on Geoscience*, 12 (2), p.145-162. DOI: [10.17014/ijog.12.2.145-162](https://doi.org/10.17014/ijog.12.2.145-162)

INTRODUCTION

This time, land throughout the world will experience erosion towards the ocean due to coastal erosion by seawater on the coast (Zhu *et al.*, 2019). The coastline has sand and soil, which is always

moist with seawater (Hassan *et al.*, 2021). The land surface does not always form a flat plane, or have elevation differences between one place and another, thus forming a slope (Sadeghian, 2022). The slope is a topographic condition that is often found in various civil construction works (Khatun *et al.*,

2019). Slopes can occur naturally or be deliberately created by humans for certain purposes (Löfroth *et al.*, 2021). The slope referred to, in this research, is the coast, which occurs due to excessive coastal water overflowing, resulting in continuous erosion.

Coastal areas are dynamic environments formed by interactions between land and sea, thus providing challenges for infrastructure development and environmental management (Sriyanto *et al.*, 2022). Understanding coastal slope stability is critical to reducing erosion, protecting coastal assets, and ensuring public safety (Chen *et al.*, 2020). The shear strength of the soil determines the resistance of coastal slopes to collapse, while the forces caused by waves exert significant pressure on the slope, thereby affecting the stability of the slope (Ghafooripour *et al.*, 2012). By combining a geotechnical analysis of soil properties with the assessment of wave-induced forces, this research seeks to provide a comprehensive understanding of coastal slope behaviour. The coastal slopes sometimes experience landslides toward the sea due to high tides (Masi *et al.*, 2021). Landslides are a natural disaster that often occurs on natural and artificial slopes (Lamens and Askarinejad, 2021). Slope failures mostly occur during the rainy season, due to the increased pore water pressure on the slope. This results in a decrease in soil shear strength and internal friction angle, which then causes landslides (Mukhlisin *et al.*, 2022).

A slope stability analysis has a very important role in planning civil constructions (Rossi *et al.*, 2021). Unstable slopes are very dangerous for the surrounding environment, therefore, a slope stability analysis is very necessary. Meanwhile, the measure of slope stability is known by calculating the magnitude of the safety and sustainability factors (Khanmohammadi and Razavi, 2024). Through the integration of soil shear strength analysis and wave-induced force calculations, the motivation to do this research is to develop a better method for assessing the coastal slope stability by increasing the understanding of complex interactions between soil properties and wave dynamics.

The research methodology used Bea and Audibert's (1980) which is a simple approach to analyse the slope stability under the influence of

wave loads. Whilst, previous research has used many other methods, such as the limit equilibrium method or the finite element method, to assess the slope stability and to design coastal structures. Most previous studies have also included analysis of wave characteristics such as height, period, and direction in calculating wave-induced forces on coastal slopes. However, these studies focus on integrating hydrodynamic factors with geotechnical parameters to better understand the complex interactions between soil shear strength and wave pressure. Research such as that conducted by Zheng *et al.* (2019) used MATLAB to calibrate load and resistance factors on slope foundations and breakwaters, and developed a more reliable programme for the stability analysis. The research by Sin *et al.* (2022) studied the influence of earthquake events and rainfall on the slope stability in various regions, linking an increase in pore water pressure with a decrease in soil shear strength, which can trigger landslides. The study by Chen *et al.* (2020) integrated a numerical model to evaluate the stability of wave-affected submarine slopes, providing an in-depth perspective on the interaction between ground shear forces and wave pressure.

The new approach in the research using the coastal slope stability methods under wave loading conditions by Bea and Audibert (1980), was regretted by (Kraft *et al.*, 1982). This research differentiates itself from other research through a more integrated, efficient approach, and a focus on coastal dynamics. While many other studies focus on more complex methods or single aspects, where this research stands out for the use of a simple method capable of providing results that can be implemented directly in the field, and still considers the complex factors of the interaction between land and waves. This method serves as a framework for assessing the slope stability, while wave characteristics such as height, period, and direction are considered to calculate the driving forces caused by waves. This research aims to optimise the stability of coastal slopes by integrating analysis of soil shear strength with calculations of force due to waves. This research contributes to the development of sustainable coastal management strategies and resilient coastal infrastructure (Chen *et al.*, 2020).

This research aims to evaluate the interaction between the slope stability and wave dynamics, with a focus on the forces acting on coastal slopes and their response to shear and driving forces.

METHODS AND MATERIALS

This systematic approach integrates hydrodynamic and geotechnical analyses to assess the slope stability and to inform coastal engineering practice. Through numerical modelling and empirical methods, it improves the understanding of wave-coastal slope interactions and contributes to effective strategies for coastal resilience and risk mitigation (Dey and Basudhar, 2008; Setiady, 2010; Muthukumar *et al.*, 2022).

The methodology for analyzing the coastal slope stability under wave loading conditions consists of six main steps: wave characteristics analysis, geotechnical location investigation, driving force calculation, resisting force calculation, factor of safety (*FoS*) analysis, and soil shear strength analysis. By using a simplified slope stability analysis method by Bea and Audibert (1981), this research is expected to be able to calculate the Factor of Safety (*FoS*) of slopes. The research flow can be described sequentially, which means that the research steps are aligned with the results (Sukma *et al.*, 2022). The research steps can be seen in Figure 1.

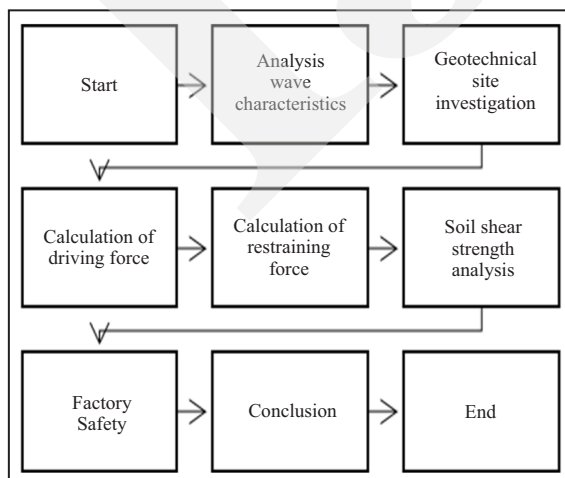


Figure 1. Research steps.

Based on Figure 1, this research step can be divided into six process stages:

1. Analysis of wave characteristics that includes examining the height, period, and direction of waves to determine the intensity and spatial distribution of the forces generated by waves on the coastal slope, using historical data or numerical models (Hassan *et al.*, 2021). Calculating wave shear stress on the seabed used horizontal wave speed (*U*).

$$\tau = \frac{1}{2} \times \gamma \omega \times Hc \times U^2 \dots\dots\dots(1a)$$

$$U = \frac{Hc}{T} \dots\dots\dots(1b)$$

The calculation of wave shear stress considered the angle between the wave direction and the direction perpendicular to the seabed (θ):

$$\tau = \frac{1}{2} \times \gamma \omega \times Hc \times \cos(\theta) \dots\dots\dots(1c)$$

where:

- τ is wave shear stress units (kN/m²),
- $\gamma \omega$ is the water density in units (kN/m³),
- Hc* is the sig wave height in length units (m),
- U* is the horizontal speed of the wave, for linear waves in units (m/s)
- T* is the wave period in period units (s)

2. Geotechnical site investigations, focussing on characterising the properties of seabed sediments through soil sampling and laboratory tests, to obtain parameters such as cohesion, friction angles, and unit weight, which are important for the subsequent stability analysis. This method utilizes Atterberg indices, such as the liquid limit and plastic limit, to estimate soil cohesion (Milošević *et al.*, 2020). Meanwhile, "k" refers to the wave friction coefficient or other variables related to the hydrodynamic forces acting on coastal slopes. Further explanation regarding the context and definition of this parameter needs to be included to clarify its role in analysing the slope stability under wave loads. To calculate this, the following formula was used:

$$c = k \cdot (LL - PL) \dots\dots\dots(2a)$$

This research also used the Consistency Method. This formula is based on the results of measuring the consistency or strength of the soil. To calculate this, the following formula was used:

$$c = k \cdot \sqrt{Su} \dots\dots\dots(2b)$$

where:

- c is the cohesion (units kN/m²),
- k is the wave friction coefficient,
- LL is the liquid limit,
- PL is the plastic limit,
- Su is the soil's undrained strength

To calculate the pore water pressure amplitude u and the effective normal stress amplitude, the following formula were used (Yamamoto, 1981)

$$u = \rho_0 \cdot e^{-\lambda z} \dots\dots\dots(3a)$$

$$\sigma v = \sigma h = \tau v h = \rho_0 \cdot \lambda \cdot z e^{-\lambda z} \dots\dots\dots(3b)$$

where:

- u is the pore pressure,
- p is the pressure,
- h is the depth in units (meters),
- σ is the effective normal stress

3. Driving force calculations quantify the magnitude and distribution of pressure due to waves using empirical or analytical formulas based on wave characteristics and seabed geometry (Zheng *et al.*, 2019). The formula for wave pressure is unique:

$$P\omega = \frac{1}{2} \gamma \omega \cdot Hc \cdot H \dots\dots\dots(4a)$$

The formula for driving force:

$$W = (\gamma \cdot H) + P\omega \dots\dots\dots(4b)$$

where:

- W is the driving force in force units (kN/m),
- $\gamma\omega$ is the water density in units (kN/m³),
- $P\omega$ is the wave pressure units (N/m²),
- Hc is the sig wave height in length units (m),
- h is the depth in units (m)

4-5. Resisting force calculations to evaluate the ability of the soil to resist shear deformation under wave-loading conditions, and taking into account cohesive and frictional forces along potential failure surfaces (Ghafooripour *et al.*, 2012) used the formula for soil shear force:

$$\tau_{soil} = (\gamma \cdot H \cdot L \cdot \sin(\beta) \cdot \tan(\phi)) \dots\dots\dots(5)$$

where:

- τ is wave shear stress units (kN/m²)
- γ is the water density in force units (kN/m³)
- L is the slope width (m)
- h is the depth units (m)
- β is the slope angle in angle units (degrees)
- Φ is the friction angle units (degrees)

While the formula for resisting forces:

$$R = c \cdot A + (\gamma \cdot H \cdot L \cdot \sin(\beta) \cdot \tan(\phi)) \dots\dots\dots(6)$$

$$R = \text{Soil Cohesion} + \text{Soil Shear Force} \dots\dots\dots(7)$$

where:

- R is the resisting force (units kN/m),
- and A is the slope area (m³)

6. Factory of Safety (FoS) analysis determines the stability conditions by calculating the ratio of resisting force to driving force (Chen *et al.*, 2020). FoS is greater than unity means stability, whereas if it is less than unity, it indicates potential instability, which requires corrective action. The calculation of Factor of Safety (FoS):

$$FoS = \frac{R}{W} \dots\dots\dots(8)$$

where:

- R is the resisting forces (units kN/m),
- and W is the driving force in force units (kN/m)

The calculation of soil shear strength ($\hat{c}u$):

$$\sigma' = \sigma - u \dots\dots\dots(9)$$

$$\hat{c}u = c' + \sigma' \cdot \tan(\phi) \dots\dots\dots(10)$$

where:

- c is the cohesion (units kN/m²),
- cu is the soil shear strength (kN/m²),
- σ is the effective normal stress

The important parameters are used in calculating the driving force and resistance force in the slope stability analysis. The authors explain that these parameters serve as input for various equations related to the interaction between land and sea waves. Wave shear stress measured in kN/m^2 is the horizontal force produced by ocean waves acting on the seabed. Driving force, measured in kN/m , is the force that drives a slope to move or slide, caused by wave pressure and gravity. Wave horizontal velocity (U) measures the speed of waves on the sea surface in m/s , which plays an important role in calculating the driving force. Soil cohesion (c) and internal friction angle (Φ): These two parameters are very important for calculating the soil resistance force. Soil cohesion provides additional resistance to driving forces, while the internal shear angle determines how much the soil can withstand shear stress. Factor of Safety (FoS) is the ratio of the resistance force to the driving force. If the FoS value is greater than one, the slope is considered stable. Conversely, if FoS is less than one, the slope has the potential to collapse.

The samples used in this research were Core Borehole Log (BH)= twenty-six samples and Cone Penetration Test (CPT)= twenty-four samples

RESULT AND ANALYSIS

In this section, the research results will be discussed based on the stages that have been determined. The results of this research can be explained as follows:

Analysis of the Characteristics of this Wave Includes

Homogeneous soil with constant properties throughout the slope and infinite slope geometry (*i.e.* two-dimensional analysis), in this research, used as an infinite slope geometry approach, considered as an effective method for analysing the slope stability, especially in conditions where the slope can be imagined as two dimensions with length greater than depth. Terzaghi's approach to measuring effective stress was applied

to analyze the interaction between sea waves and coastal slopes, by considering changes in pore water pressure that influence soil shear strength. Skempton and DeLory's method (1957) for calculating undrained shear strength was applied to assess the slope stability under the influence of wave shear forces, which significantly influence the pore water pressure on coastal slopes. The Bea and Audibert (1979) method was applied to calculate the influence of waves on the slope stability in coastal areas, especially in the context of the driving force of waves acting on infinite slopes. Infinite slope geometry modelling was used in this research because this approach is suitable for analysing long and shallow coastal slopes. The coastal slope in the studied area can be assumed to be two-dimensional, where the length of the slope is much greater than its depth.

Assumed Plane Failure Surface (Generally Assumed to be Circular or Plane)

Evaluation of the driving forces that can cause coastal slope failure is critical in understanding the slope stability under the influence of waves, rainfall, gravity, and other environmental factors. These driving forces result from various sources such as ocean waves, gravity, and changes in pore water pressure, all of which can influence the soil stability on coastal slopes. In this research, the Bishop method (1955) was applied to calculate the driving force resulting from waves and pore water pressure, as well as to assess the potential of slope failure by calculating the ratio between driving force and resisting force (FoS). In this research, the evaluation of driving forces on coastal slopes was carried out by taking into account a combination of gravity, pore water pressure, and wave forces. Using the approach of Terzaghi (1943), Bishop (1955), Bea and Audibert (1979), the driving force was calculated as part of the analysis of the balance of forces acting on the slope. This research shows that the driving force of waves plays a major role in the slope instability, especially at certain depths where wave pressure peaks. Quantification of pressure due to waves and shear stress acting on coastal slopes, identify spatial variations in driving

forces along the slope profile, and analysis of the influence of wave characteristics on the magnitude and distribution of the driving force.

Assessment of the Opposing Forces of Cohesion Parameters that Contribute to Soil Stability

In determining soil cohesion parameters, friction angles, and unit weight from geotechnical investigations, the samples used in this research were Core Borehole Log (BH) = twenty-six samples and Cone Penetration Test (CPT) = twenty-four samples. Calculation of cohesive and frictional forces in the soil mass that resist slope failure was carried out.

Evaluating the contribution of soil properties to overall slope stability under wave loading conditions comprises a calculation of safety factors (FoS) that influence the safety of coastal slopes, calculation the resisting force (shear strength) and driving force (gravity) acting on the slope, determining the Factor of Safety (FoS) using the equation $FoS = \text{Resisting Force}/\text{Driving Force}$. FoS greater than 1 indicates a slope stability, while FoS less than 1 indicates instability condition.

Selecting Failure or Failure Surfaces, Slope Geometry, and Soil Properties

Selecting an appropriate failure, commonly used failure surface shapes include circular, flat, or noncircular types, depending on the slope morphology and loading conditions, including exploration of the sensitivity of slope stability and FoS values to changes in wave characteristics, soil properties, and slope geometry. The activity also to identify important factors that influence the slope stability under wave loading conditions.

In this research, the stability of coastal slopes was analyzed using a slope geometry approach and identification of failure areas that are influenced by soil properties and external forces such as waves and gravity.

Slope Geometry Model.

The geometric model used in this research is the infinite slope, where the slope is idealised

as two dimensions. This approach was chosen because coastal slopes often have a length that is much greater than their depth, so this model is suitable for describing actual conditions in the field. The slope geometries used include slope angle (β), where slopes were analyzed by considering the angle of the slope, measured horizontally. This angle affects the stability of the slope because the steeper the slope, the greater the driving force of gravity acting on the slope. Slope depth (h) was calculated from the land surface to the seabed, which influences the distribution of driving forces and soil shear forces. Slope surface area (A) is the slope along the horizontal profile that was analyzed to evaluate the distribution of acting forces, both from gravity and waves.

Failure Analysis Model

The failure plane on coastal slopes is usually influenced by soil properties, external forces, and environmental conditions. The failure analysis was carried out by taking into account the driving forces of waves and gravity, as well as the physical properties of the soil that contribute to the soil resistance to these forces.

Failure Field Selection Model

Planar Failure Surface

A flat failure plane is often to be assumed on slopes with granular soil (such as sand) or sandy soil. These fields usually appear along straight lines that follow the gradient of the slope. In this case, the driving force of the wave tends to act in the same direction as gravity, and causes the ground to slide linearly. Planar failure usually occurs when the shear force acting on the soil exceeds the shear capacity of the soil.

Curved/Circular Failure Surface

For clay or cohesive soils, a failure often occurs along a curved plane, called a circular failure plane. These fields result from a rotational landslide mechanism, where the soil moves along a curve. In the case of cohesive soil, the driving forces of waves and gravity cause rotation of the soil mass along a curved line. Circular failure

planes were analysed using methods such as the Bishop method or Janbu method (1973), which measures the ratio of driving force to resistance force to determine the failure potential.

Non-circular Failure Field

Some conditions can cause irregular or non-circular failure planes, especially if the slope has complex geometric variations or a combination of cohesive and non-cohesive soils. Non circular failure planes often appear on slopes that have soil heterogeneity, where soil layers with different strengths interact in a complex manner under the influence of wave and gravitational forces.

Selection of Failure Plane, Slope Geometry, and Soil Properties

The choice of failure plane is highly dependent on the soil properties found at the researched location as well as the geometry of the slope. Based on field data and laboratory analysis, several important aspects that must be considered are:

- Internal shear angle (ϕ). This is an important parameter in determining the capacity of the soil to resist driving forces. Soils with higher angles of internal friction tend to be more stable and have greater resistance to failure.
- Soil cohesion (c). Soil cohesion plays a major role in resisting driving forces. Cohesive soils, such as clay, have higher cohesion compared to sand, so they are more resistant to failure, especially in curved failure areas.
- Soil density. Denser soils tend to be more resistant to failure due to greater resistance forces. Soil density at the studied location was evaluated through laboratory testing and used to calculate soil resistance forces.

Shear Strength Parameters to Analyse Coastal Slope Stability

To determine shear strength parameters such as cohesion (c) and friction angles (ϕ), as well as soil specific gravity (γ), soil shear stress ($\hat{c}u$) are performed in laboratory or field test. These parameters are important inputs for calculating

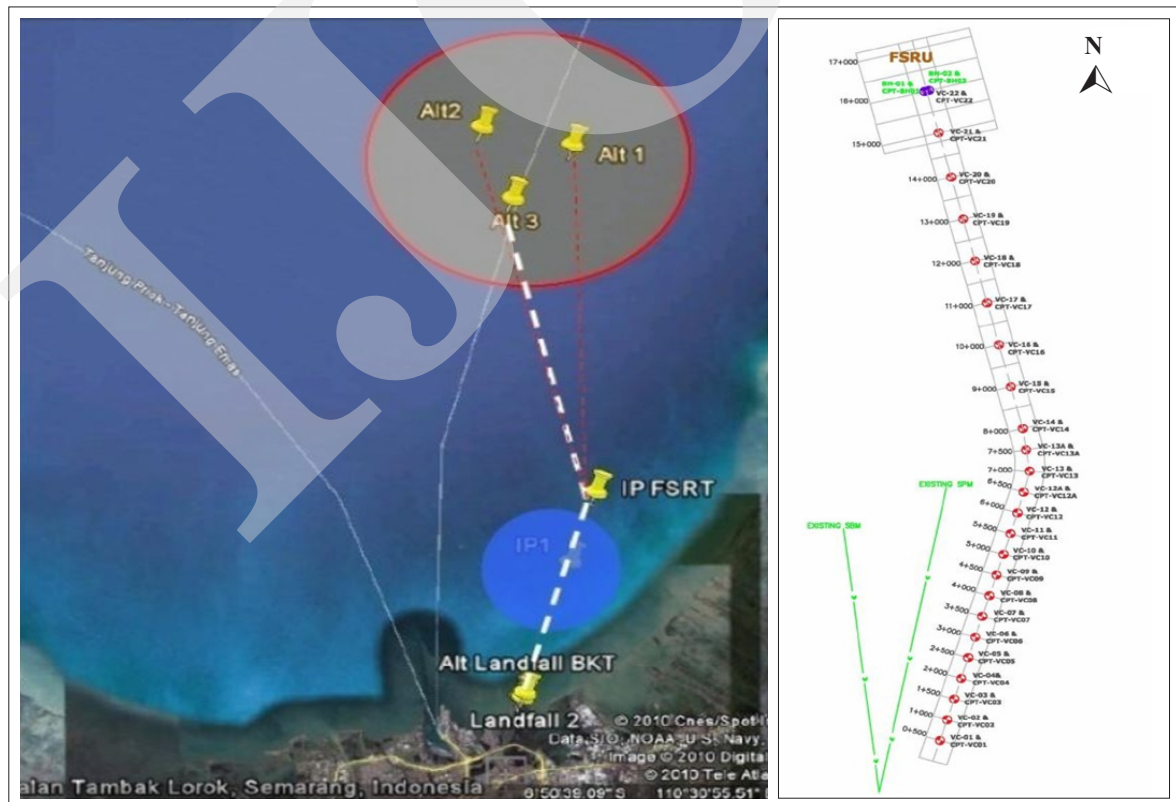


Figure 2. Research location map.

the resisting force in a stability analysis, as shown in Figure 2.

The surveyed area located on the north coast of Central Java, around 16 km from the Port of Tanjungmas - Semarang (Figure 2) consists of a proposed pipeline route corridor approximately 16 km long and 800 m wide, and 2.4 km x 2.4 km of the proposed FSRU area. The purpose of the survey along the proposed pipeline route is to determine whether there are any hazards to the installation and operation of the proposed pipeline. The minimum water depth within the proposed FSRU area is 20.0 m LWS.

As part of the overall survey works, the purpose of the geotechnical survey is not only to conduct a desk study, but also to collect soil data necessarily to support the conceptual design for selecting type and location of the FSRU, as well as pipe routing. Geotechnical survey points on the pipe route and FSRU were plotted on two samples consisting of Core Borehole Log (BH)= twenty-six samples, and Cone Penetration Test (CPT)= twenty-four samples. The soil weight can be seen in Table 1.

Table 1 categorises soil based on soil density (γ) in units of kN/m^3 , which is an important parameter for calculating the effective normal pressure on the soil. This data was taken at a certain depth, which was then used in the slope stability analysis. A homogeneous wave shear stress was considered with the following properties, those are Water density (γ_w): 9.81 kN/m^3 (water standard value), Significant Wave Height (Hs): 1.5 m, (T): 8.0 (seconds), and Wave Length (L): 82.24 m. The properties of wave shear stress can be calculated as wave shear stress, horizontal wave speed on the seabed with significant waves, using Equations 1a and 1b. The calculation of

shear stress, horizontal wave speed on the seabed with a significant wave:

$$U = \frac{1.5 \text{ m}}{8 \text{ sec}} = 0.19$$

$$\tau = \frac{1}{2} \times 9.81 \text{ kN/m}^3 \times 1.5 \text{ m} \times (0.19)^2$$

$$\tau = 0.597 \text{ kN/m}^2$$

Based on the above analysis and the use of formulas, the pressure amplitude, wave pressure, effective normal stress, and driving force analysis can be determined as presented in Table 2. Meanwhile, the retaining force, safety factor analysis, and soil shear strength is shown in Table 3.

Table 2 presents the results of calculating the effective normal stress and driving force on the coastal slope at various depths, *i.e.* Effective Normal Stress (σ): This is the force acting vertically on a slope caused by the weight of the soil and pore water pressure, functioning as is a key parameter to determine how stable a slope is under the influence of waves; and Wave Pressure (P): Measured in kN/m^2 , produced by waves pushing up a slope from the seaside. The increase in pressure with depth can increase the driving force acting on the slope.

According to Table 3, Resistance Force (R) is a force that resists soil movement produced by cohesion and internal friction of the soil. This table presents the resistance force values at different depths. The table shows that *FoS* fluctuates with depth, where lower values are found at greater depths, indicating potential slope instability.

Based on Tables 2 and 3, to make it easier to see the results of this research, the correlation can be seen in Figure 3.

Table 1. Soil Weight

(c) Cohesion (kN/m)				(γ) Soil Weight (kN/m3)			
0.00-0.75	0.75-1.50	1.50-2.25	2.25-3.00	0.00-0.75	0.75-1.50	1.50-2.25	2.25-3.00
(m) below seabed							
2.501	2.562	2.979	3.199	3.45	3.72	3.70	3.70

Table 2. Pressure Amplitude, Wave Pressure, Effective Normal Stresses, and Driving Force Analysis

Depth (m)	(p0) Pressure amplitude (kN/m ²)	(τ)Wave Shear Stress (kN/m ²)	(PW) Wave pressure (kN/m ²)							(σ) Effective normal stresses (kN/m ²)							(W) Driving Force (kN/m ²)						
			0.00-0.75	0.75-1.50	1.50-2.25	2.25-3.00	0.00-0.75	0.75-1.50	1.50-2.25	2.25-3.00	0.00-0.75	0.75-1.50	1.50-2.25	2.25-3.00	0.00-0.75	0.75-1.50	1.50-2.25	2.25-3.00					
2.1	7.2683	7.1453	15.451	20.969	26.487	32.005	1.248	1.491	1.704	1.889	22.696	31.571	39.807	48.100									
3.4	7.1275	7.2182	25.016	30.534	36.052	41.570	1.618	1.806	1.970	2.110	36.746	45.972	54.182	62.475									
4.3	6.9953	7.2584	31.637	37.155	42.674	48.192	1.807	1.962	2.096	2.209	46.472	55.941	64.134	72.427									
4.7	6.9283	7.2908	34.580	40.098	45.617	51.135	1.875	2.017	2.138	2.240	50.795	60.372	68.557	76.850									
5.0	6.8748	7.3092	36.788	42.306	47.824	53.342	1.919	2.051	2.164	2.258	54.038	63.696	71.874	80.167									
5.4	6.7996	7.3184	39.731	45.249	50.767	56.285	1.970	2.091	2.192	2.276	58.361	68.127	76.297	84.590									
5.9	6.6996	7.3232	43.409	48.927	54.446	59.964	2.023	2.128	2.217	2.289	63.764	73.665	81.826	90.119									
6.4	6.5934	7.3266	47.088	52.606	58.124	63.642	2.062	2.154	2.231	2.292	69.168	79.204	87.354	95.647									
6.9	6.4818	7.3291	50.767	56.285	61.803	67.321	2.089	2.170	2.235	2.287	74.572	84.743	92.883	101.176									
7.5	6.3412	7.3303	55.181	60.699	66.218	71.736	2.108	2.175	2.228	2.269	81.056	91.389	99.518	107.811									
8.1	6.1945	7.3313	59.596	65.114	70.632	76.150	2.112	2.167	2.209	2.241	87.541	98.036	106.152	114.445									
8.5	6.0938	7.3333	62.539	68.057	73.575	79.093	2.108	2.155	2.191	2.217	91.864	102.467	110.575	118.868									
8.8	6.0169	7.3354	64.746	70.264	75.782	81.300	2.102	2.144	2.175	2.196	95.106	105.790	113.892	122.185									
9.2	5.9129	7.3366	67.689	73.207	78.725	84.243	2.089	2.124	2.149	2.166	99.429	110.221	118.315	126.608									
10.0	5.7004	7.3360	73.575	79.093	84.611	90.129	2.050	2.073	2.089	2.096	108.075	119.083	127.161	135.454									
10.8	5.4839	7.3355	79.461	84.979	90.497	96.015	1.996	2.010	2.017	2.017	116.721	127.945	136.007	144.300									
12.6	4.9912	7.3338	92.705	98.223	103.741	109.259	1.836	1.834	1.826	1.814	136.175	147.885	155.911	164.204									
14.3	4.5319	7.3328	105.212	110.730	116.249	121.767	1.656	1.644	1.628	1.610	154.547	166.716	174.709	183.002									
16.0	4.0899	7.3319	117.720	123.238	128.756	134.274	1.465	1.448	1.428	1.406	172.920	185.548	193.506	201.799									
17.5	3.7202	7.3318	128.756	134.274	139.793	145.311	1.299	1.279	1.257	1.234	189.131	202.164	210.093	218.386									
18.9	3.3956	7.3320	139.057	144.575	150.093	155.611	1.150	1.129	1.107	1.084	204.262	217.673	225.573	233.866									
20.1	3.1341	7.3326	147.886	153.404	158.922	164.440	1.030	1.009	0.987	0.965	217.231	230.966	238.842	247.135									
21.4	2.8688	7.3329	157.451	162.969	168.487	174.005	0.909	0.889	0.868	0.847	231.281	245.367	253.217	261.510									
22.5	2.6590	7.3336	165.544	171.062	176.580	182.098	0.815	0.795	0.776	0.756	243.169	257.552	265.380	273.673									

Table 3. Resisting Forces, Factor of Safety Analysis, and Soil Shear Strength Analysis

Depth (m)	Soil Shear Force (kN/m ²)						(R) Resisting Forces (kN/m ²)						(FoS) Factor of Safety						(Cu) Soil Shear Strength (kN/m ²)					
	0.00-0.75	0.75-1.50	1.50-2.25	2.25-3.00	3.00-3.75	3.75-4.50	0.00-0.75	0.75-1.50	1.50-2.25	2.25-3.00	3.00-3.75	3.75-4.50	0.00-0.75	0.75-1.50	1.50-2.25	2.25-3.00	3.00-3.75	3.75-4.50	0.00-0.75	0.75-1.50	1.50-2.25	2.25-3.00	3.00-3.75	3.75-4.50
2.1	0.029	0.044	0.057	0.065	0.065	0.065	2.530	2.606	3.036	3.265	3.265	0.111	0.083	0.076	0.068	0.068	0.068	2.562	2.638	3.067	3.293	3.293	3.293	
3.4	0.047	0.064	0.077	0.085	0.085	0.085	2.548	2.626	3.056	3.284	3.284	0.069	0.057	0.056	0.053	0.053	0.053	2.580	2.654	3.081	3.304	3.304	3.304	
4.3	0.060	0.078	0.091	0.098	0.098	0.098	2.560	2.640	3.070	3.298	3.298	0.055	0.047	0.048	0.046	0.046	0.046	2.589	2.662	3.087	3.309	3.309	3.309	
4.7	0.065	0.085	0.098	0.104	0.104	0.104	2.566	2.647	3.077	3.304	3.304	0.051	0.044	0.045	0.043	0.043	0.043	2.592	2.664	3.090	3.310	3.310	3.310	
5.0	0.069	0.089	0.102	0.109	0.109	0.109	2.570	2.651	3.081	3.308	3.308	0.048	0.042	0.043	0.041	0.041	0.041	2.595	2.666	3.091	3.311	3.311	3.311	
5.4	0.075	0.096	0.109	0.115	0.115	0.115	2.576	2.658	3.088	3.314	3.314	0.044	0.039	0.040	0.039	0.039	0.039	2.597	2.668	3.092	3.312	3.312	3.312	
5.9	0.082	0.103	0.117	0.122	0.122	0.122	2.582	2.665	3.095	3.322	3.322	0.041	0.036	0.038	0.037	0.037	0.037	2.600	2.670	3.094	3.313	3.313	3.313	
6.4	0.089	0.111	0.125	0.130	0.130	0.130	2.589	2.673	3.103	3.329	3.329	0.037	0.034	0.036	0.035	0.035	0.035	2.602	2.672	3.095	3.313	3.313	3.313	
6.9	0.096	0.119	0.132	0.137	0.137	0.137	2.596	2.681	3.111	3.337	3.337	0.035	0.032	0.033	0.033	0.033	0.033	2.603	2.672	3.095	3.312	3.312	3.312	
7.5	0.104	0.128	0.142	0.146	0.146	0.146	2.605	2.690	3.121	3.346	3.346	0.032	0.029	0.031	0.031	0.031	0.031	2.604	2.673	3.094	3.312	3.312	3.312	
8.1	0.112	0.137	0.151	0.155	0.155	0.155	2.613	2.699	3.130	3.355	3.355	0.030	0.028	0.029	0.029	0.029	0.029	2.604	2.672	3.093	3.310	3.310	3.310	
8.5	0.118	0.144	0.158	0.161	0.161	0.161	2.618	2.706	3.136	3.361	3.361	0.029	0.026	0.028	0.028	0.028	0.028	2.604	2.672	3.092	3.309	3.309	3.309	
8.8	0.122	0.148	0.162	0.166	0.166	0.166	2.623	2.710	3.141	3.365	3.365	0.028	0.026	0.028	0.028	0.028	0.028	2.603	2.671	3.092	3.308	3.308	3.308	
9.2	0.128	0.155	0.169	0.172	0.172	0.172	2.628	2.717	3.147	3.371	3.371	0.026	0.025	0.027	0.027	0.027	0.027	2.603	2.670	3.090	3.306	3.306	3.306	
10.0	0.139	0.167	0.181	0.184	0.184	0.184	2.639	2.729	3.160	3.383	3.383	0.024	0.023	0.025	0.025	0.025	0.025	2.601	2.667	3.087	3.303	3.303	3.303	
10.8	0.150	0.179	0.194	0.196	0.196	0.196	2.650	2.741	3.173	3.395	3.395	0.023	0.021	0.023	0.024	0.024	0.024	2.598	2.664	3.083	3.299	3.299	3.299	
12.6	0.175	0.207	0.222	0.223	0.223	0.223	2.675	2.769	3.201	3.423	3.423	0.020	0.019	0.021	0.021	0.021	0.021	2.590	2.655	3.074	3.289	3.289	3.289	
14.3	0.198	0.234	0.249	0.249	0.249	0.249	2.699	2.796	3.228	3.448	3.448	0.017	0.017	0.018	0.019	0.019	0.019	2.582	2.646	3.063	3.279	3.279	3.279	
16.0	0.222	0.260	0.276	0.274	0.274	0.274	2.722	2.822	3.255	3.474	3.474	0.016	0.015	0.017	0.017	0.017	0.017	2.572	2.636	3.053	3.269	3.269	3.269	
17.5	0.243	0.283	0.300	0.297	0.297	0.297	2.743	2.845	3.278	3.496	3.496	0.015	0.014	0.016	0.016	0.016	0.016	2.564	2.627	3.044	3.260	3.260	3.260	
18.9	0.262	0.305	0.322	0.318	0.318	0.318	2.763	2.867	3.300	3.517	3.517	0.014	0.013	0.015	0.015	0.015	0.015	2.557	2.619	3.036	3.253	3.253	3.253	
20.1	0.279	0.324	0.341	0.336	0.336	0.336	2.779	2.886	3.319	3.535	3.535	0.013	0.012	0.014	0.014	0.014	0.014	2.551	2.613	3.030	3.247	3.247	3.247	
21.4	0.297	0.344	0.361	0.355	0.355	0.355	2.797	2.906	3.340	3.555	3.555	0.012	0.012	0.013	0.014	0.014	0.014	2.545	2.607	3.024	3.241	3.241	3.241	
22.5	0.312	0.361	0.378	0.372	0.372	0.372	2.813	2.923	3.357	3.571	3.571	0.012	0.011	0.013	0.013	0.013	0.013	2.541	2.602	3.019	3.237	3.237	3.237	

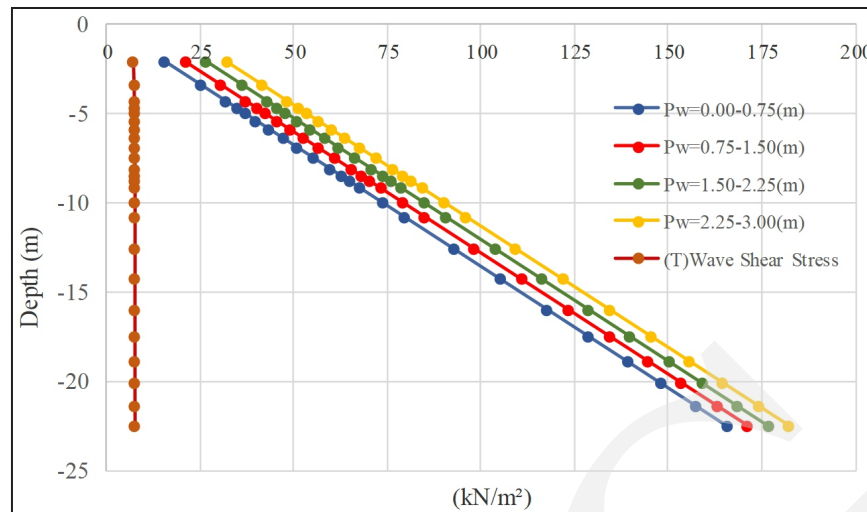


Figure 3. Graphs indicating wave shear stress-wave pressure.

Figure 3 explains the relationship between wave shear stress and wave pressure with the following graphic, *i.e.* the blue, red, green, and yellow lines represent the wave pressure distribution at different depths ($P_w = 0.00-0.75$ m, $P_w = 0.75-1.50$ m, $P_w = 1.50-2.25$ m, $P_w = 2.25-3.00$ m, respectively). These lines show how wave pressure decreases with increasing depth. Brown lines and dots represent Wave Shear Stress. This shear stress also decreases with increasing depth, and the trend of these points is different compared to wave stress.

Based on Figure 3, wave shear stress plays a role in causing horizontal movement and tends to influence the lateral shear of the soil. Meanwhile, wave pressure acts vertically and can cause vertical movement or compression, contributing to a decrease in shear strength due to the increased pore water pressure. Explanations regarding brown dots on graphs or diagrams are usually used to mark the location of important data or certain measurement points. This can include points along the slope surface or in areas where certain forces (such as shear stress or pressure). The brown line may represent a trend or profile of the data showing changes in a parameter, such as wave pressure or driving force, along a slope or depth. This line helps in depicting the changing trend of a variable in the context of the study. Wave pressure measurements at the surface may not reflect deeper changes occurring below the ground surface. Therefore, significant

increases may occur at certain depths, but are not detectable at the surface. By comparing these two values, it can be seen that although the shear stress of waves tends to be relatively constant or only increases slightly with depth, wave pressure increases significantly. This suggests that hydrostatic pressure forces from waves may have a greater impact on slope stability than shear forces, especially at deeper depths. The wave shear stress driving force can be seen in Figure 4.

Figure 4 explains the wave shear stress driving force with the following graphic: the blue, red, green, and yellow lines represent the thrust distribution at different depths ($W = 0.00-0.75$ m, $W = 0.75-1.50$ m, $W = 1.50-2.25$ m, $W = 2.25-3.00$ m, respectively). These lines illustrate how the thrust changes with increasing depth. The light blue lines and dots depict Wave Shear Stress. This shear stress decreases with depth, but the trend of these points appears different compared to the thrust force.

Based on Figure 4, these two values are compared. It can be seen that there is a correlation between wave shear stress and thrust force. The wave shear stress increases as the thrust force increases. This shows that the wave force plays a role in producing a larger thrust force, which in turn can increase the potential for material movement on the slope. It is, on the contrary, there is a significant difference between the two values. This may indicate the existence of other factors that

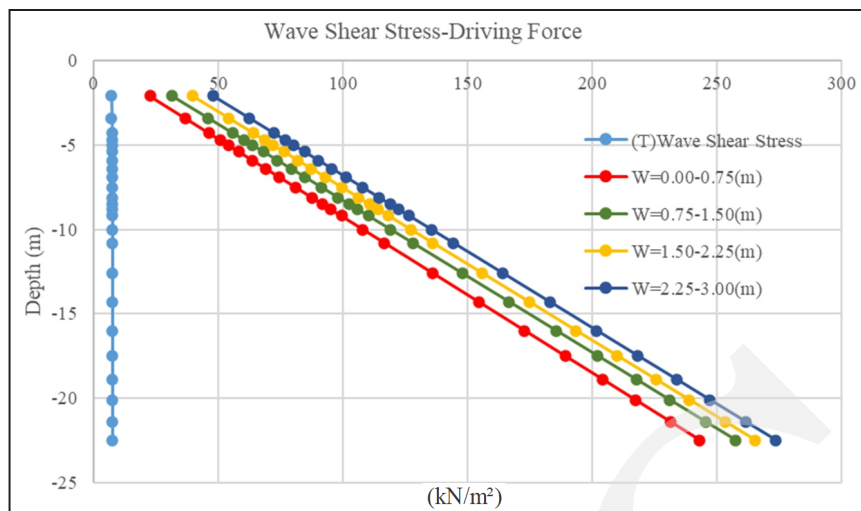


Figure 4. Graphs showing wave shear stress-driving force.

influence the distribution of forces on the seabed and the potential for the movement of material on the slope. The blue colour pointing downwards on the graph probably represents wave shear stress (Figure 4). This usually indicates that horizontal forces acting on the ground due to wave movement, which can affect the slope stability. The blue dots and lines are indicated with the notation "W", which shows that they relate to wave-induced shear forces, effective normal stress soil shear strength shown in Figure 5.

Figure 5 explains the relationship between wave-induced shear forces and effective normal stress soil shear strength with the following

graphic: Blue, red, green, and yellow lines representing variations in Effective Normal Stress (σ') at different depths. This effective normal stress value shows how much force is applied to the soil grains below the surface as depth increases. Whilst orange, light green, light blue, and brown lines and dots indicate Soil Shear Strength (c_u'), or the shear strength of the soil, at various depths. This value shows how much the soil can withstand shear forces before failure occurs.

Moreover, Figure 5 shows that the slope tends to be stable at that depth. On the contrary, if the shear strength of the soil exceeds the effective normal pressure, slopes may be susceptible to

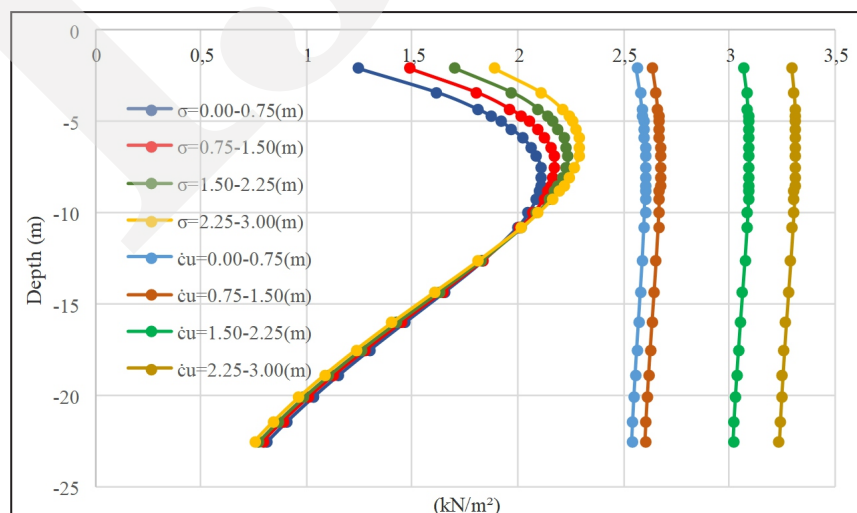


Figure 5. Graphs indicating effective normal stress-soil shear stress.

shifting or failure. However, effective normal pressure tends to decrease with depth. The shear strength of the soil remains relatively consistent. This shows that at that depth, pushing forces tend to be smaller than resisting forces, which indicates that the slope at that depth is stable or has the potential for high stability. The slope tends to be stable at a certain depth where the soil shear strength (which is indicated by the shear parameter) is greater than the effective normal pressure (Figure 5). At this point, the slope is in a safe condition, and the risk of failure is relatively low. On the other hand, if the shear strength of the soil begins to decrease and is no longer able to compensate for the effective normal pressure, the slope becomes vulnerable to displacement or failure. The effective normal pressure limit taken from the graph can be determined by finding the value at which the soil shear strength and the effective normal pressure intersect. This point is an important indicator for analyzing potential failure effective normal stress driving force that is shown in Figure 6.

Furthermore, Figure 6 displays the potential failure effective normal stress driving force with the following graphic: The blue, red, green, and brown lines on the left of the graph show the Effective Normal Stress (σ') acting at a certain depth. This effective normal stress describes the pressure exerted on the soil as depth increases. The light blue, light green, yellow, and orange

lines show the Driving Force (W) values at various depths. This driving force is the force that encourages ground movement or slope failure.

Based on Figure 6 and by comparing these two values, the balance between pushing and resisting forces on a slope can be evaluated. If the effective normal pressure is greater than the thrust force, as seen at a depth of 2 m, the slope tends to be more stable. However, if the driving force is dominant, as occurs at a depth of 22.5 m, slopes may be susceptible to failure due to the dramatic increase in thrust forces. Another factor that can strengthen the slope stability is extensive root strengthening, which is the most relevant to the slope stability (Masi *et al.*, 2021). The driving force of the resistance force can be seen in Figure 7. The figure explains the driving force of the resistance force with the following graphic. This figure shows that the driving force and resistance force decrease linearly with increasing depth. This indicates that the driving force and resistance forces are influenced by the depth. The deeper the soil or water, the force will decrease proportionally. The difference in lines based on wave width (W) and resistance level (R) shows that the greater the wave width or resistance, the greater the force generated at any given depth.

According to Figure 7 and by comparing these two values, the stability of the slope under the influence of the acting forces can be evaluated.

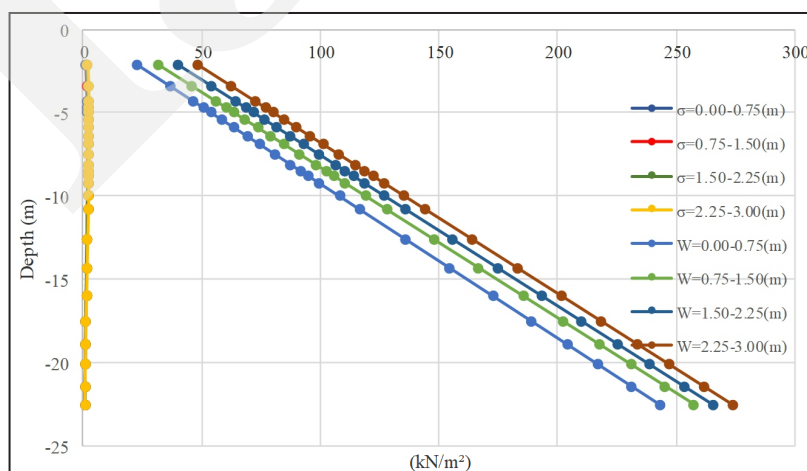


Figure 6. Graphs showing effective normal stress-driving force.

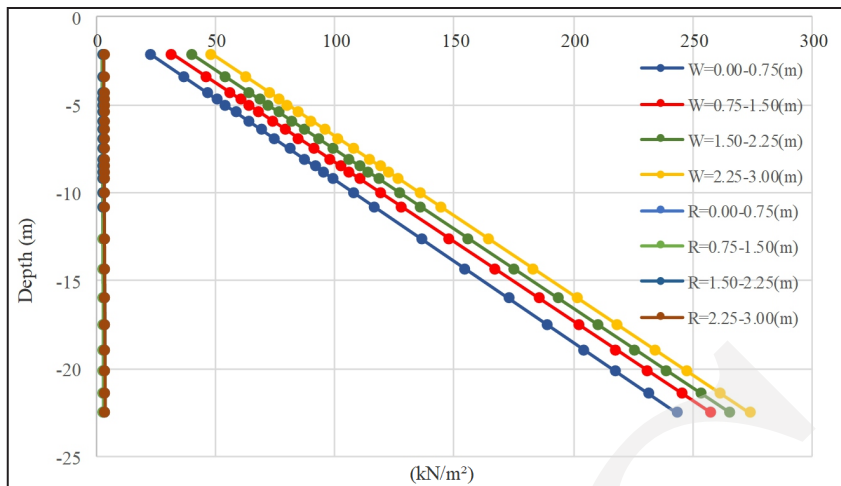


Figure 7. Graphs indicating driving force-resistant force.

If the pushing force is greater than the resistance force, as occurs at a depth of 22.5 m, slopes may be susceptible to failure due to an imbalance in these forces. On the contrary, if the resistance force is greater than the pushing force, as occurs at a depth of 2 m, slopes tend to be more stable due to the soil's ability to withstand greater shifts or deformations. The soil shear force and soil shear strength presented in Figure 8. The figure 8 explains the soil shear force and soil shear strength with the following graphic. The graph shows the comparison between shear force (cf) and shear strength (cu) at various depths. The cf (shear force) tends to be on the left side of

the graph with small values (below 1 kN/m²), indicating that the shear force acting on the soil is relatively low throughout the depth. Higher cu (shear strength), shown on the right side of the graph (approximately 2.5 kN/m² to 3.5 kN/m²), indicates that the soil has a greater capacity to resist shear forces.

Based on Figure 8 and by comparing these two values, the potential for ground movement on the slope can be evaluated. If the soil shear force is greater than the soil shear strength as occurs at a depth of 22.5 m, the possibility of ground shifting increases due to an imbalance in these forces. On the contrary, if the soil shear

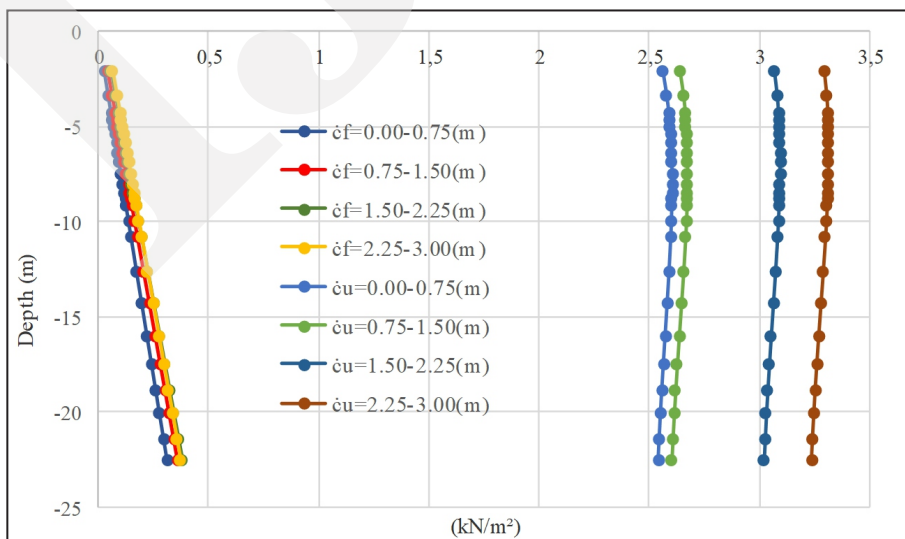


Figure 8. Graphs showing soil shear force-soil shear strength.

strength is greater than the soil shear force. as occurs at a depth of 2 m, the probability of soil shifting may be lower due to the soil ability to resist shifting or deformation. The factor of safety regarding the potential for slope failure occurs in Figure 9, explaining the factor of safety regarding the potential for slope failure with the following graphic. The graph shows that the FoS value increases with increasing depth. At surface depths of about 0 to -5 m, FoS values start from about 0.02 and increase gradually to nearly 0.1 at deeper depths. The largest FoS values of around 0.1 to 0.12 are achieved at depths of around -20 m and below, indicating that the soil at these depths has a greater capacity to withstand applied forces compared to shallower depths.

Based on Figure 9, the calculated Factor of Safety (FoS) is more than 1, indicating a stable condition where the restraining force far exceeds the driving force. In the slope stability analysis, FoS represents the margin of safety against slope failure, which is calculated as the ratio of the resisting force to the driving force (Ghafooripour *et al.*, 2012; Sin, Azmi, and Ghasemi, 2022). At a depth of 2 m, it produces an FoS value of 0.111. while at a depth of 22.5 m, the FoS value decreases to 0.012. This difference indicates a significant shift in the balance between resistance and thrust forces at greater depths. A change from 0.111 to 0.012 indicates a drastic reduction in slope stability. This change is more than 100

% (almost to zero) and is very significant in the context of the stability analysis. On the other hand, if the change in FoS from 0.111 to 0.001 is more than 0.001, then this supports the argument about a very significant decrease in stability. When FoS decreases below 0.1, an FoS value of 1 is usually considered as the stable limit. That is, if the FoS is greater than 1, the slope is considered stable. While if FoS is less than 1, the slope is considered unstable. In this case, the value of 0.012 at a depth of 22.5 m indicates that the slope is in a very unstable condition, and the risk of ground shifting is very high. Therefore, the change in FoS value from 0.111 at a depth of 2 m to 0.012 at a depth of 22.5 m is not only significant but also indicates extreme instability conditions at deeper depths.

If the driving force is dominant and exceeds the ability of the resisting force to resist slope movement, the slope may be in an unstable condition, and require mitigation measures to prevent potential failure. Other researches refer to geophysicists to ensure the slope stability in an area, namely with FoS slope classification charts made from seismic refraction data (U. Aka *et al.*, 2022). Based on the research results, a thorough understanding of the interactions between these factors is needed to identify potential risks of slope failure and to formulate appropriate mitigation strategies (Schmüdderich *et al.*, 2022).

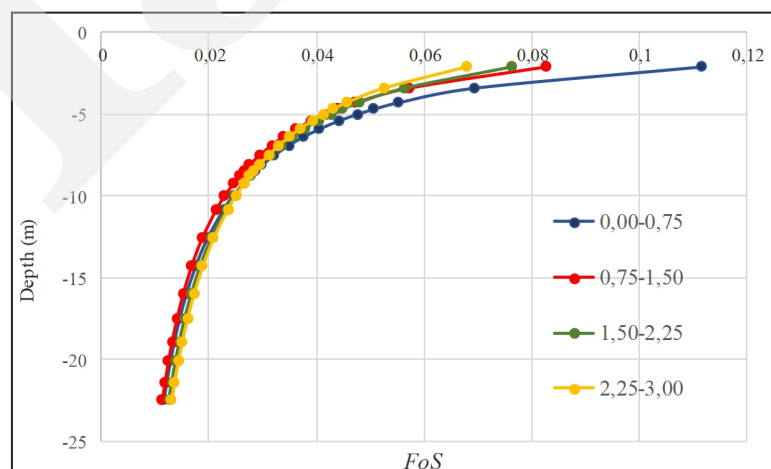


Figure 9. Graphs showing factor of safety.

DISCUSSION

The gap analysis in this study mainly focuses on the interaction between the slope stability and wave dynamics. Analyzed data produce a balance between various forces acting on the slope, and stress on the comparison between various parameters related to the slope stability. Meanwhile, other researchers use methodologies such as the limit balance method and the finite element method of stability analysis. The focus is broader on soil shear strength analysis and calibration of load and resistance factors on slope foundations and breakwaters, and involves the analysis of the development and validation of programme reliability on the MATLAB platform (Zheng *et al.*, 2019). So overall, both studies have the same goal, namely understanding and assessing slope stability, but differ in terms of specific methodology, focus areas, and depth analysis carried out.

In the context of this research, the choice of failure plane is very dependent on the physical properties of the soil, pore water pressure, and the influence of wave forces. For soils with low shear angles and high cohesion, circular failure planes are more likely to occur (Khatun *et al.*, 2019). On the other hand, for granular soils such as sand, failure is more likely to occur along a flat failure plane, where the driving forces of gravity and waves act in the same direction and cause linear soil movement (Rossi *et al.*, 2021). This approach provides a deeper understanding of how slope geometry and soil properties influence the coastal slope stability under wave influence. Using data from laboratory tests and established stability analysis methods, this research successfully evaluated the potential for slope failure and provided recommendations for mitigating the risk of failure.

The innovations introduced in this research provide a more dynamic and comprehensive framework for assessing slope stability in coastal areas. By integrating wave dynamics with soil shear strength analysis, this research bridges the gap in traditional models that often ignore the complex interactions between waves and

soil properties. Detailed examination of driving forces and resistance forces, combined with depth-specific *FoS* analysis, provides coastal engineers with valuable insights into reducing the risk of slope failure, making this research highly relevant for sustainable coastal management and infrastructure resilience.

CONCLUSIONS

Based on data analysis and data processing carried out on several key parameters related to the slope stability and the influence of waves on it, several conclusions can be drawn.

1. Comparison between effective normal pressure and soil shear strength. The balance between pushing and resisting forces on a slope can be evaluated by comparing the effective normal pressure with the soil shear strength. If the effective normal pressure is greater than the thrust force, then the possibility of slope stability increases.
2. Comparison between wave shear stress and wave pressure. This comparison can provide an understanding of the distribution and intensity of the forces acting on the seabed, which is important for evaluating the potential influence of waves on the slope stability.
3. Comparison between thrust force and resistance force. Comparative analysis between thrust force and resistance force can provide an idea of slope stability. If the pushing force is greater than the resistance force, then the slope may be susceptible to failure.
4. Comparison between soil shear force and soil shear strength. Comparing soil shear force with soil shear strength can provide information about the potential for soil movement on a slope, which is important for evaluating the possibility of ground shifting and slope stability.
5. Relationship between wave shear stress and thrust force. This analysis can provide insight into the potential for material movement on slopes, especially if there is a correlation be-

tween the distribution of forces on the seabed and the pushing force exerted by waves.

6. Factor of Safety (*FoS*) Analysis. The factor of safety is the ratio between the resistance force and the thrust force. If *FoS* is greater than one, then the slope is considered stable. However, if *FoS* is less than one, the slope may be unstable and require mitigation measures.

ACKNOWLEDGMENTS

In this section, the researcher would like to thank all parties including the Padjadjaran University who have facilitated this research. Colleagues from the same class have provided motivation and support, so that this research can be completed quickly.

REFERENCES

- Aka, M., Moses, M.M., Ekpa, C.I., Effiong, A.D., Osu, J.C., and Ibuot, J., 2022. Integration of Seismic Refraction and Laboratory Test Techniques for Slope Stability Analysis, South-South, Nigeria. *Earth Science Malaysia*, 6 (1), p.50-55. DOI: 10.26480/esmy.01.2022.50.55.
- Bea, R.G. and Audibert, J.M.E., 1980. Offshore platforms and pipelines in Mississippi River delta. *Journal Geotechnical Engineering Division, Proceedings American Society Civil Engineering*, 106 (GT8), p.853-869.
- Chen, W., Liu, C., Li, Y., Chen, G., Jeng, D., Liao, C., and Yu, J., 2020. An integrated numerical model for the stability of artificial submarine slope under wave load. *Coastal Engineering*, 158 (October 2019). DOI: 10.1016/j.coastaleng.2020.103698.
- Dey, A. and Basudhar, P., 2008. Stability of submarine slopes subjected to wave forces and external loadings. *Aygec*, p.301–310.
- Ghafooripour, A., Niroumand, H., Faizi, K., Nazir, R., Kassin, K.A., Loon, T., Adhami, B., and Moayed, H., 2012. Slope stability of the design concept of the sheet pile and contiguous bored pile walls. *Archives Des Sciences Journal*, 65 (4), 2
- Hassan, M.A., Ismail, M.A.M., and Shaalan, H.H., 2021. Numerical Modeling for the Effect of Soil Type on Stability of Embankment. *Civil Engineering Journal (Iran)*, 7, p.41-57. DOI: 10.28991/CEJ-SP2021-07-04.
- Khanmohammadi, M. and Razavi, S., 2024. Proposing New Artificial Intelligence Models to Estimate Shear Wave Velocity of Fine-grained Soils : A Case Study. *International Journal of Engineering Journal*, 37 (06), p.1164-1174. DOI: 10.5829/ije.2024.37.06c.13.
- Khatun, S., Ghosh, A., and Sen, D., 2019. An experimental investigation on effect of draw-down rate and drawdown ratios on stability of cohesionless river bank and evaluation of factor of safety by total strength reduction method. *International Journal of River Basin Management*, 17 (3), p.289-299. DOI: 10.1080/15715124.2018.1498856.
- Lamens, P. and Askarinejad, A., 2021. Pile driving and submarine slope stability: a hybrid engineering approach. *Landslides*, 18 (4), p.1351-1367. DOI: 10.1007/s10346-020-01585-2.
- Löfroth, H., O'Regan, M., Snowball, I., Holmén, M., Kopf, A., Göransson, G., Hedfors, J., Apler, A., and Frogner-Kockum, P., 2021. Challenges in slope stability assessment of contaminated fibrous sediments along the northern Baltic coast of Sweden. *Engineering Geology*, 289 (5), p.1-16. DOI: 10.1016/j.eng-geo.2021.106190.
- Masi, E.B., Segoni, S., and Tofani, V., 2021. Root reinforcement in slope stability models: A review. *Geosciences (Switzerland)*, 11 (5), p.1-24. DOI:10.3390/geosciences11050212.
- Milošević, M., Logar, M., and Djordjević, B., 2020. Mineralogical analysis of a clay body from Zlakusa, Serbia, used in the manufacture of traditional pottery. *Clay Minerals*, 55 (2), p.142-149. DOI: 10.1180/clm.2020.20.
- Mukhlisin, M., Hamdani, B., Novita, E., Sukoyo, and Rabinah, A.H., 2022. Behaviour of Friction Resistance of Pile Groups on Clay Soil During Loading Tests: Case Study in Semarang and Temanggung, Central Java,

- Indonesia. *Indonesian Journal on Geoscience*, 9 (1), p.61-69. DOI: 10.17014/ijog.9.1.61-69.
- Muthukumar, S., Kolathayar, S., Valli, A., and Sathyan, D., 2022. Pseudostatic analysis of soil nailed vertical wall for composite failure. *Geomechanics and Geoengineering*, 17 (2), p.561-573. DOI: 10.1080/17486025.2020.1827163.
- Rossi, N., Bačić, M., Kovačević, M.S., and Librić, L., 2021. Development of fragility curves for piping and slope stability of river levees. *Water (Switzerland)*, 13 (5), p.1-19. DOI: 10.3390/w13050738.
- Sadeghian, M., 2022. The Reliability Assessment of a Ship Structure under Corrosion and Fatigue, using Structural Health Monitoring. *International Journal of Engineering Journal*, 35 (9), p.1765-1778. DOI: 10.5829/ije.2022.35.09c.13.
- Schmüdderich, C., Machaček, J., Prada-Sarmiento, L.P., Staubach, P., and Wichmann, T., 2022., *Strain-dependent slope stability for earthquake loading*. *Computers and Geotechnics*, 152, 10548. DOI: 10.1016/j.compgeo.2022.105048.
- Setiady, D., 2010. Hubungan Kumpulan Mineral Berat pada Sedimen Pantai dan Lepas Pantai dengan Batuan Asal Darat di Perairan Teluk Pelabuhan Ratu , Jawa Barat. *Indonesian Journal on Geoscience*, 5 (1), p.57-74. <http://ijog.bgl.esdm.go.id>.
- Sin, G.C., Azmi, M., and Ghasemi, M., 2022. Evaluation of Slope Stability Due to Earthquake and Rainfall Occurrences. *Home Proceedings of AWAM International Conference on Civil Engineering*, 3 (1), p.368-378.
- Sriyanto, S.P.D., Angmalisang, P A., and Manu, L., 2022. Optimal Tide Gauge Location for Tsunami Validation in The Lembeh Island, North Sulawesi. *Indonesian Journal on Geoscience*, 9 (3), p.315-327. DOI: 10.17014/ijog.9.3.315-327.
- Sukma, D.I., Prabowo, H.A., Setiawan, I., Kurnia, H., and Maulana, I., 2022. Implementation of Total Productive Maintenance to Improve Overall Equipment Effectiveness of Linear Accelerator Synergy Platform Cancer Therapy. *International Journal of Engineering*, 35 (07), p.1-11. DOI: 10.5829/IJE.2022.35.07A.05.
- Yamamoto, T., 1981. Wave-Induced Pore Pressures and Effective Stresses in Inhomogeneous Seabed Foundations. *Ocean Engineering*, 8, p.1-16.
- Zheng, D. F., Nian, T. K., Bo, L., Liu, M., Yin, P., and Huo, D. Y., 2019. Investigation of the stability of submarine sensitive clay slopes under wave-induced pressure. *Marine Georesources and Geotechnology*, 37 (1), p.116-127. DOI: 10.1080/1064119X.2018.1481470.
- Zhu, J.F., Chen, C.F., and Zhao, H.Y., 2019. An approach to assess the stability of unsaturated multilayered coastal-embankment slope during rainfall infiltration. *Journal of Marine Science and Engineering*, 7 (6), p.1-20. DOI: 10.3390/jmse7060165.